

7

42717

FERMILAB

JUL 28 1997

ANL-HEP-CP-97-48

LIBRARY

The Atmospheric Neutrino Flavor Ratio in Soudan 2

Maury Goodman
For the Soudan 2 Collaboration

HEP362, Argonne National Lab, Argonne Ill. 60439, USA

Abstract. The Soudan 2 collaboration has measured the atmospheric neutrino flavor ratio with 2.63 kiloton years of exposure. Our measured flavor ratio is $0.67 \pm 0.15(\text{stat}) + 0.04-0.06(\text{syst})$. The neutrino induced horizontal muon flux has been measured to be $\Phi_\mu = (4.12 \pm 1.1 \pm 0.58) \times 10^{-13} \text{cm}^{-2} \text{sr}^{-1} \text{s}^{-1}$.

I INTRODUCTION

The measurement of the atmospheric neutrino flavor ratio is of interest due to the apparent anomaly by some reported experiments [8,5,7,1,3] and the possible explanation of that anomaly in the context of neutrino oscillations. The double ratio

$$R \equiv \left(\frac{\nu_\mu}{\nu_e} \right)_{\text{data}} / \left(\frac{\nu_\mu}{\nu_e} \right)_{MC} \sim \left(\frac{\text{tracks}}{\text{showers}} \right)_{\text{data}} / \left(\frac{\text{tracks}}{\text{showers}} \right)_{MC}$$

allows a measurement which is independent of an absolute flux or exposure calculation.

Soudan 2 is an iron calorimeter with different experimental systematics from the water Cherenkov detectors and whose geometry and detection technique differ from the Frejus experiment. A large veto shield placed against the cavern wall allows the identification of particles entering the detector from the interactions of cosmic ray muons in the surrounding rock. We used these "rock" events to determine whether our low value of R could be due to contamination from such events.

II DETECTOR AND EXPOSURE

The 963 metric ton Soudan 2 experiment is located in the Soudan Underground Mine State Park, Minnesota, 710 meters underground. About 85% of

Conference paper submitted to the proceedings of the Sixth Conference on the Intersections of Particle and Nuclear Physics, May 27 - June 2, 1997.

The submitted manuscript has been authored by a contractor of the U. S. Government under contract No. W-31-109-ET. Accordingly, the U. S. Government retains a nonexclusive, royalty-free license to reproduce the published form of this contribution, or allow others to do so, for U. S. Government purposes.

ANL-HEP-CP-97-48



the mass is provided by 1.6 mm thick sheets of corrugated steel. The sheets are stacked to form a hexagonal 'honeycomb' structure. Plastic drift tubes (1.0 m long and 15 mm in diameter) fill the spaces in the honeycomb. An 85% argon/15% CO₂ gas mixture is recirculated through the modules. Ionization deposited in the gas drifts toward the closer end of the tube in an 180 volt/cm electric field. The drift velocity is approximately 0.6 cm/ μ sec, which yields a maximum drift time of 83 μ sec. The average density is 1.6 g/cc. Further details of module construction may be found in Reference [2].

The calorimeter is surrounded by a 1700 m² active shield designed to detect charged particles which enter or exit the detector cavern. The shield covers about 97% of the total solid angle. The basic element is an extruded aluminium manifold, consisting of eight hexagonal proportional tubes arranged in two layers of four. A two-layer coincidence is required to signal a high energy particle entering or leaving the cavern. The measured efficiency of a coincidence is 95%. Details of the shield performance can be found in Reference [11].

III DATA REDUCTION

We have analyzed data from 2.63 fiducial kton-year exposure taken between April 1989 and March 1995. During this period the detector was under construction, starting with a total mass of 275 tons and ending with the complete 963 tons. There were 75 million triggers taken. The goal of the data reduction is to obtain a sample of 'contained events', defined as those in which no primary particle in the event enters or leaves the fiducial volume of the detector. The fiducial volume is defined by a 20 cm depth cut.

The events are passed through a software filter to reject events with tracks entering or leaving the fiducial volume (mostly cosmic ray muons) or events which have the characteristics of radioactive background or electronic noise. Approximately 1 event per 1500 triggers passes this filter.

The selected events are then double scanned to check containment and to reject background events, using an interactive graphics program. The main backgrounds are residual radioactive and electronic noise, badly reconstructed cosmic ray muons, and events where muons pass down the gaps between individual modules, either finally entering a module and stopping or interacting in material in the gap and sending secondary tracks into the modules. Any event with a track which starts or ends on a gap, or which can be projected through a gap to the exterior of the detector is rejected. In addition, events with a vertex in the crack region are rejected. Differences between scanners are resolved by a second level scan. Approximately 1 event in 40 passed by the program filter is finally selected as contained. The average efficiency of individual scanners in selecting contained events was 93.5%. Further details of the event selection procedure can be found in Reference [9].

IV NEUTRINO MONTE CARLO

Monte Carlo events equivalent to 5.9 times the exposure of the real data were inserted randomly into the data stream and processed simultaneously with the data events, ensuring that they are treated identically. The neutrinos were generated using the BGS flux [4]. The variation of the ν intensity with the solar cycle was corrected using neutron monitor data [9,6].

At the low ν energies characteristic of the atmospheric flux the predominant interactions are quasi-elastic or resonance production. Full details of the event generation process and a detailed comparison with all available low energy data are given in Reference [9]. Nuclear physics effects were represented by the Fermi gas model. Rescattering of pions within the nucleus was applied using data obtained by comparison of bubble chamber ν interactions on deuterium and neon [10]. Particles produced in the neutrino interactions were tracked through the detector geometry using the EGS and GEISHA codes. The generated event was superimposed on a pulser trigger which reproduces noise and background in the detector as they vary with calendar time.

V EVENT CLASSIFICATION

The lepton flavour of each event is determined by the second level scanners who flag them as 'track', 'shower' or 'multiprong'. Single track events which have heavy ionization and are straight are separately classified as 'proton'. Proton recoils accompanying tracks and showers are an additional tag of quasi-elastic scattering and are ignored in the classification. Any second (non-proton) track or shower in the event results in a multiprong classification. Results are shown in Table 1. Events without (with) shield hits are labeled "gold" ("rock") events. As a test of the systematic uncertainties introduced by the classification process, all scanning was done independently by two groups prior to merging for the final results.

TABLE 1. Classifications for the contained events before corrections.

	Track	Shower	Multiprong	Proton
Data: gold	75	106	89	22
Data: rock	237	312	177	130
MC	461	445	432	48

The quality of the flavour assignment was measured using the Monte Carlo data. Table 2 shows the fraction of Monte Carlo events selected as contained which were classified in each category. It can be seen that 87% of events

assigned as tracks have muon flavour and 96% of showers electron flavour. The ratio of accepted muon to electron charged current Monte Carlo events is approximately 1:1, different from the ratio of 2:1 for the $\pi \rightarrow \mu \rightarrow e$ decay chain. At these low energies threshold effects due to the difference in the muon and electron masses cause the generated event ratio to be approximately 1.5:1. Acceptance differences for high energy muons and electrons and the cuts required to remove background produced by cosmic ray muons passing down the gaps between modules further reduce the ratio.

TABLE 2. Monte Carlo identification matrix.

Generated	Track	Assigned		
		Shower	Multiprong	Proton
ν_μ cc	0.87	0.01	0.38	0.24
ν_e cc	0.05	0.96	0.44	0.04
Neutral current	0.08	0.03	0.18	0.72

VI BACKGROUND SUBTRACTION

The majority of the 1148 events classified as contained are due to the interactions of neutral particles (neutrons or photons) produced by muon interactions in the rock around the detector. Calculations show that only a few percent of such events will not have an accompanying charged track traversing our shield, which was placed as close to the cavern wall and as far away from the detector as possible to maximize the probability of detecting the accompanying charged particles. The efficiency of the shield has been measured using single cosmic ray muons detected in the main detector. It ranges from 81% during the early data runs before the geometrical coverage was complete to 93% at the end of this data period. Also, 8.9% of pulser events overlaid on Monte Carlo events had a random shield coincidence.

Our large sample of rock events enables us to investigate muon induced background by studying the depth distribution of the events in the detector. This allows us to simultaneously measure any backgrounds due to either shield inefficiency or contained events due to neutral particles entering the detector without being accompanied by charged particles in the shield. Neutrino events should be distributed uniformly throughout the detector, while background events are attenuated towards the center. We define a measure of the proximity of the event to the detector exterior by calculating the minimum perpendicular distance from the event vertex to the detector edge.

The depth distribution for tracks and showers from the gold, rock and neutrino Monte Carlo samples are shown in Figure 1. The points are the gold data, the shaded histogram is the neutrino Monte Carlo, normalized to the

experiment exposure, and the unshaded histogram is the rock data, normalized to the same number of events as the data sample. It can be seen that the data more closely resembles the neutrino depth distribution than the rock background depth distribution. In the next section, we fit the shape of the gold data to the shapes of the neutrino Monte Carlo and rock samples to estimate the rock background. This produces a noticeable error in the flavor ratio obtained due to the statistics of the fit, but this is required to properly take into account the possibility of background contributions to the flavor ratio.

VII CALCULATION OF R

In using the depth distribution of the rock events to correct for background, we note that the measured flavor ratio as a function of shield multiplicity is observed to be a constant value of 0.76 ± 0.07 . We then correct the track to shower ratio in the data by fitting the track and shower depth distribution to a sum of those in the rock events and Monte Carlo, constraining the flavor ratio of the rock events to its observed value. The result of the fit is 20.4 tracks and 26.9 showers in the gold sample are due to background, leading to a corrected neutrino induced rate of 54.6 tracks and 79.1 showers. From this we calculate $R = 0.67 \pm 0.15$, where the error includes the statistical error on the data, the statistical error on the Monte Carlo, and the error on the background subtraction from the fit.

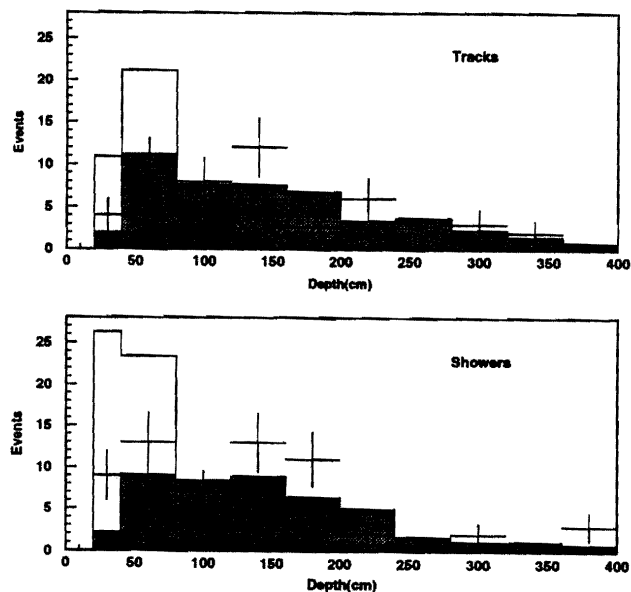


FIGURE 1. *The depth distributions for tracks (top) and showers (bottom)*

Systematic errors have been calculated based on errors on the flux models, neutrino cross sections, scanning, and the assumption that the flavor ratio of the background is independent of shield multiplicity. The latter systematic error, which can be measured by fitting the tracks and showers separately, leads to an asymmetric error. We calculate a total systematic error on R of $+0.04$ and -0.06 .

VIII HORIZONTAL NEUTRINO INDUCED MUON FLUX

Soudan 2 cannot resolve upward from downward going muons. But using horizontal muons, where the atmospheric muon contribution is significantly diminished, we can isolate neutrino induced throughgoing muons. The slant depth calculation uses U.S.G.S. digitized surface elevation data. Muon events which have a slant depth in excess of 14 km.w.e. are considered to be from the population of muons induced from atmospheric neutrinos. Acceptance to this population of muons varies slightly with zenith owing to topographical effects on the surface. The solid angle acceptance for this slant depth starts near 81 degrees, includes all of solid angle beyond 83 degrees, and totals 1.77 sr. The effective solid angle was calculated by Monte Carlo to be 84.86 m^2 . Trigger and program efficiencies have been estimated to be 81%. The initial search has produced 14 events which pass the 175 cm track-length cut corresponding to a muon energy threshold of 600 MeV. The calculated flux is $\Phi_\mu = (4.12 \pm 1.1 \pm 0.58) \times 10^{-13} \text{ cm}^{-2} \text{ sr}^{-1} \text{ s}^{-1}$. This matches the expected flux using our 600 MeV threshold.

IX CONCLUSIONS

We have measured the flavour ratio of ratios (R) in atmospheric neutrino interactions using a 1.52 kton-year exposure of Soudan 2. We find $R = 0.67 \pm 0.15_{-0.06}^{+0.04}$. This value is about 2σ from the expected value of 1.0 and is consistent with the anomalous ratios measured by the Kamiokande and IMB experiments. We note that since our acceptance matrix is different from those of the water Cherenkov experiments we would not expect to measure the same value of R , unless $R=1$.

REFERENCES

1. M. Aglietta et al., *Europhys. Lett.* **8**, 611 (1989).
2. W.W.M. Allison et al., *NIM A* **376**, 36 (1996).
3. W.W.M. Allison et al., *Physics Lett.* **B391**, 491 (1997).

4. G. Barr et al., G. Barr, T.K. Gaisser and T. Stanev, Phys Rev **D39**, 3532 (1989).
 5. R. Becker-Szendy et al., Phys. Rev. **D46**, 3720 (1992).
 6. b J. Beiber, Bartol Research Institute, private communication.
 7. K. Daum et al., Z. Phys. **C66**, 417 (1995).
 8. Y. Fukuda et al., Phys. Lett. **B335**, 237 (1994).
 9. H. Gallagher, H. Gallagher, Neutrino Oscillation Searches with the Soudan 2 detector, PhD Thesis, University of Minnesota (1996).
 10. R. Merenyi et al., Phys. Rev. **D45**, 743 (1992).
 11. W.P. Oliver et al., NIM **A276**, 371 (1989).
-